

Original Research

L-type (Loaf) Cervical Secretion Crystallization Directionality Biomarker Study

José María Murcia Lora^{1,*}, María Luisa Esparza Encina², Cristina Reig³,
Oscar Martínez Martínez⁴, Jennifer Simoni⁵, María Ángeles Martínez Calvo⁶,
Juan Luis Alcázar⁷

¹Department of Restaurative Reproductive Medicine, Clinical Consulting G&E, Logroño, 26002 La Rioja, Spain

²Department of Endocrinology and Restaurative Reproductive Medicine, Clinical Consulting G&E, Logroño, 26002 La Rioja, Spain

³Department of Natural Family Planning, Fertility Awareness Monitor Consulting, 28003 Madrid, Spain

⁴Department of Computer Science Engineering Logroño, University of La Rioja, 26006 La Rioja, Spain

⁵School of Medicine, University of Navarra, 31008 Pamplona, Spain

⁶Department of Materials Science and Engineering, University of La Rioja, 26006 Logroño, Spain

⁷Department of Obstetrics and Gynecology, Clínica Universidad de Navarra, 31003 Pamplona, Spain

*Correspondence: clinicalconsultinggye@gmail.com (José María Murcia Lora)

Academic Editor: Luca Roncati

Submitted: 21 November 2022 Revised: 23 February 2023 Accepted: 23 March 2023 Published: 14 June 2023

Abstract

Background: Cervical discharge is considered a hydrogel, which is part liquid and part solid. Under physiological conditions, the characteristic “fern-leaf” arborization is proportional to the circulating estradiol concentration and maximal in the preovulatory phase. Crystallization of the cervical secretion is a process of dehydration with the arrangement of sodium and potassium chloride crystals around a main axis composed of mucin. L-type (Loaf) (L) is proportional to the circulating estradiol concentration and is higher in the Fertile Window (FW). Currently, most studies comparing the FW with cervical discharge include the biophysical fertile window (BFW) which is 6 days before the estimated day of ovulation (EDO). **Methods:** Samples were taken from the vulvovaginal region within the FW using the Creighton Model System for Fertility Care (CrMS). Optical images of the samples were digitized to perform a binarization, skeletonization, and crystallization directionality study of the scanned branches. These samples taken from the vulvovaginal secretion were not collected from the endocervix. They were recorded by the Vaginal Secretion Recording System (VDRS) using CrMS. The FW was taken into account from 6 days before the peak (P) day according to CrMS. A statistical study was performed by comparing vulvovaginal crystallization samples including -6 day EDO in FW. **Results:** Out of 29 samples, 58.6% deemed true positives, 34% were true negatives, 6.8% represented 2 false positives, and no cases were false negatives ($p < 0.001$). **Conclusions:** Our analysis of the statistical distribution of the branching angles of the crystallization of cervical secretions allowed us to detect a significant contribution of 90-degree frequencies, indicating, the existence of an L-type pattern in the FW samples that we studied. The skeletonization of the studied images together with a FW indicator allowed us to identify this crystallization pattern. We therefore propose this feature detection mechanism as a novel biomarker of fertility.

Keywords: fertile window; naprotechnology; cervical secretion; ovulation; fertility awareness; subfertility; biophysical biomarkers; biotechnology; creighton model fertility care system (CrMS)

1. Introduction

Follicle Stimulating Hormone (FSH) levels increase in the follicular phase and are highest in the pre-ovulatory period, and maximum in the middle of the cycle [1]. At serum FSH concentrations between 15 to 20 mIU/mL serum estradiol rises above baseline. Subsequently, estradiol concentrations increase during the follicular phase. Thus, as the menstrual cycle progresses, estrogen stimulates the central production of FSH, and FSH in turn stimulates the production of estrogen progressively entering the bloodstream [2,3]. This is the basis for the present contribution since there is a well-documented correlation between the days of the beginning of the cycle, with stimulation of serum estradiol around 291.25 ± 8.89 pmol/L (mean \pm SEM). As

the cycle progresses, the quality of daily estrogen released by the ovaries increase, reaching levels around 701.22 ± 16.28 pmol/L, ($p < 0.0001$) [4]. FSH levels in the bloodstream are well characterized throughout the menstrual cycle [5,6]. These changes occur because the dominant follicle responds to a threshold level of FSH, which raises estrogens both systemically as well as locally in the cervix [1]. Gradual changes in the characterization of cervical secretion, are a faithful mirror of the variations of the follicular dynamics and the ovulation process. Estimates of the day of ovulation (EDO) based on basal body temperature (BBT) were reported by Barrett & Marshall in 1969 [7], Schwartz in 1980 [8], and Royston in 1982 [9]. The American Society for Reproductive Medicine (ASRM) defines Fertile Win-



dow (FW) as the first day on which oestrone-3-glucuronide (E3G) is detected in urine until the second day after the peak of luteinizing hormone (LH) [10]. Currently, most studies define the period of greatest fertility from –6 days before ovulation to the first day after ovulation, and it is in this interval that the change from infertile days to days of greatest fertility generally occurs. This is determined by the progressive increase in serum oestrone-3-glucuronide (E3G) concentrations, from the day –6 days before EDO [11–14]. Billings [15] first proposed a now commonly used method to assess the progress of the biophysical properties of cervical secretion: to infer from the analysis of the cervical secretion at the vulva, fertile or infertile conditions according to its type, as a function of its physical touch sensation, visual appearance and consistency. Many similarly observational methods have appeared in the literature, including those by Hilgers, Ferning and others [11,16–20]. Cervical discharge is a hydrogel where the liquid component is an aqueous solution of various biochemical compounds (e.g., salts, minerals, sugars, amino acids, lipids, protein chains, enzymes, etc.) and the solid component mainly glycoproteins. These components determine the main biophysical parameters of the secretion of the cervix, which give it variations in quantity, appearance, transparency, viscoelasticity, and crystallization [21–23]. Odeblad described different types of crystallization patterns of dehydrated cervical secretions obtained by endocervical examination [24]. Type E (oestrogenic) secretion is abundant during the fertile phase and easily recognizable because it is clear, watery, elastic, and easy to quantify within the fertile phase, in quantity, appearance and consistency, characteristics that support an acellular environment suitable to sperm survival and motility [25]. The secretion type G (gestagen) is scarce, thick, opaque, and cellular which blocks sperm penetration. Since stretching and transparency in an estrogenic cervical secretion increases in the preovulatory phase their measurement and characterization can be used as basic indicators of FW [14–20,24]. The internal structure of cervical secretion varies depending on the glycoprotein net that retains a liquid medium in its meshes. At the beginning and the end of the luteal cycle, the mesh diameter of the holes does not exceed 0.5 μm . During the follicular phase, it increases gradually under the effects of estrogens until it reaches a diameter between 2 μm and 5 μm in the pre-ovulatory period. Under physiological conditions, one observes that the dehydrated secretion reduces to a structure showing an arborization pattern reminiscent of “fern leaves”. This pattern appears to correlate with the concentration of circulating estradiol and is therefore more pronounced in the pre-ovulatory phase. The characteristic changes of each phase by Odeblad can only be determined and characterized by mixing percentages of the different crystallization patterns observed by microscopy and by using an endocervical approach. The daily secretion, during the pre-ovulatory period, is around 600 to 700 mg/day, and outside of that period it is 40 or 60 mg/day.

Most studies attempting to determine the FW using observations of the cervical secretion utilize similar intervals –6 days EDO [14–20,26–28]. Currently, most studies comparing FW with cervical discharge include the biophysical fertile window (BFW) [14,28].

Crystallization of the cervical discharge of the vulvovaginal secretion is a consequence of the organization of sodium and potassium chloride crystals around a main axis formed by mucin in a process of dehydration of the cervical secretion [29]. Characteristic “fern-leaf” secretion L-type is proportional to the circulating estradiol concentration, which is higher in FW, and maximal in the pre-ovulatory phase [30–32]. L mucus exhibits “fern-like” topology, with a straight or curved central axis and branches that come out at 90° angle. These branches also act as an axis for new branches, again at 90° angles [29]. G mucus does not exhibit a predetermined form. Peak (P) mucus exhibits a star-like topology with six well-defined axes with hexagonal symmetry and branches protruding from the axes at 60° angles, resulting in 6 well defined subtypes [29]. S mucus exhibits a parallel arrangement of crystals that are close together yet not joined, and there are 3 subtypes S1–S3 [29]. These 4 patterns and are their corresponding mucus types were first reported by Odeblad in 1994 [32], and these results are successful and, like those obtained by Odeblad in 1983 [22] and Menárquez and Pastor in 2003 [29]. The presence of L and P endocervical secretions has been widely documented in the FW [22,32]. Odeblad has developed the possibility of graphically estimating L-, S- and G-type crystallization patterns in endocervical samples in the menstrual cycle [24], but it was not possible to do with cervical discharge. The assessment of the FW by Creighton Model Fertility Care (CrMS) has a well-established biological basis, as the type of cervical secretion depends on estrogen concentration, which increases about 6 days before EDO [15,32–35]. The main objective of this work was to document, using computer analysis of crystallization, the possibility of pattern recognition of L-type samples obtained in vulvovaginal discharge.

2. Material and Methods

2.1 Samples for Crystallization of Vulvovaginal Discharge

More than 100 samples were collected using two fertility recognition protocols over three months beginning in February 2022. All samples were allowed to air dry at room temperature for at least 15 minutes before being labeled and stored for further study. Samples for evaluation from the vaginal discharge of cervical secretion were collected at the vulvovaginal level by the patients themselves. The protocol for the collection of vulvovaginal secretion was considered according to two protocols with which the study was initiated, according to the norms of the Billings method and according to the norms of the CrMS. Samples obtained using the Billings protocol were collected under the supervision of a qualified Billings instructor. Crystals were collected

for three months throughout the cycle. All samples were observed with an XSZ-H optical microscope (Medilan Pamplona, Navarra, Spain) at 100, 200, and 400 magnifications. Samples of poor collection quality were excluded from the study either, due to the lack of sample quality at the time of crystal observation or those in which crystallization was not observed with the optical microscope. At the time of analyzing the group of crystals according to the collection system following the Billings protocol, it was impossible to catalog the samples and include them in the study. This was because of the loss of data, both at the time of collection, about the menstrual cycle, and about the date and time of the menstrual cycle, due to the poor quality of the samples at the time of observation under the microscope. Another reason for excluding these samples was the impossibility of recognizing the fertile window due to incorrect labeling of the samples and the impossibility of recognizing whether it was a collection inside the FW or outside the FW. In this group of crystals, no digitization study was performed due to the causes mentioned above and for this reason, this group of samples was eliminated from the study. Only samples obtained in three menstrual cycles using the CrMS recording system were considered and included in the study. The patient who was finally included in the study had been trained in the CrMS model and was closely supervised during the conduct of the study.

2.2 Fertile Window and Menstrual Cycles

The first day of the cycle was defined as the first day of menstruation, and the last day of the cycle was the day before the onset of the next menstruation. FW was defined as six days before Peak (P) day according to the CrMS model. The FW interval includes the midpoint of the fertile window $[-6P - (\text{Midpoint}) - P]$. Outside the fertile window, no digitization study was performed. For the analysis of samples obtained from vaginal discharge, a 40-year-old subfertile patient with knowledge of fertility recognition using the CrMS model was finally considered. The shortest cycle was 26 days and the longest was 31 days. Three menstrual cycles were included in the study. Three records were documented according to the Vaginal Secretion Recording System (VDRS) from the observation cards of the vaginal discharge of cervical secretion with CrMS. The patient was previously evaluated for a basic fertility study, after one year of regular sexual intercourse without contraceptives. During the study, various gynecological pathologies that could affect follicular development were ruled out, such as hyperthyroidism, hypothyroidism, hyperprolactinemia, hirsutism, hyperandrogenemia, and polycystic ovary syndrome, as well as other functional causes such as anorexia, stress, or obesity. An infertility study was performed, in which no detectable causes of female infertility were documented. The tests performed included an examination of the genital tract, a transvaginal ultrasound, vaginal cytology, colposcopy, hysterosalpingography, and hormonal

monitoring of estrogens and progesterone. The medical examination also included a follicular follow-up study, which was performed at the beginning of the clinical evaluation. Signs compatible with ovulation were documented by ultrasonography, through the observation of follicular rupture and emptying, recorded by the presence of irregular walls and echo-mixed images inside the follicle, and verifying the presence of an image compatible with corpus luteum in the post-ovulatory phase. The extraction and analysis of the data obtained from the graphs were performed by a single person. The patient gave her informed consent for inclusion before participating in the study, which was carried out in strict accordance with the Declaration of Helsinki, and whose protocol was approved by the Ethics Committee of CEImLAR, Centro de Investigación Biomédica de La Rioja (CIBIR) (approval number P.I.339).

2.3 Computer Analysis: Software Implementation and Statistical Study Phase

A total of 29 captures were selected from the samples obtained by vaginal discharge. These samples were evaluated with an XSZ-H optical microscope (Medilan, Pamplona, Navarra, Spain) to mark the area of the image to be digitized. Only crystallization samples obtained within the FW were studied. Subsequently, all images were digitized with Motic Pantera digital microscope (Motic BA410E, Barcelona, Cataluña, Spain). Once the digitized image of the samples was obtained, they were transported by universal serial bus (USB) to a personal computer (PC) to be worked with the free version of public domain software IMAGEJ/1.53h, developed at National Institute of Health and Laboratory for Optical and Computational Instrumentation (University of Wisconsin), Madison, WI, USA. This program was used for orientation, binarization, and skeletonization of all images as shown in Fig. 1.

The first step consisted of scanning the digitized image with the program, as shown in Fig. 1a. Subsequently, the sample was binarized as shown in Fig. 1b. Finally, to proceed to the study of the branches it was necessary to skeletonize the image as shown schematically in Fig. 1c. A schematic of how this last step was performed is shown in Fig. 1c. With the skeletonized image as shown in the schematic in Fig. 1c, it was possible to study the number of branches chosen with their terminal branches to determine the angles formed between them as seen in the schematic in Fig. 1c. At least 22 joints between branches and their ends were studied. To understand the procedure in this scheme, 22 junctions between branches (fuchsia) and 24 branch ends (purple) have been colored. To proceed to the study of the mean directionality in the absolute value of the junctions between branches, the component of the Fourier function was used. Finally, the angles obtained were plotted in frequency histograms and represented by a colored disk, as shown in Fig. 1d. A Chi-Square statistical study was performed with SPSS 20.0 (IBM Corp., Chicago, IL, USA) to

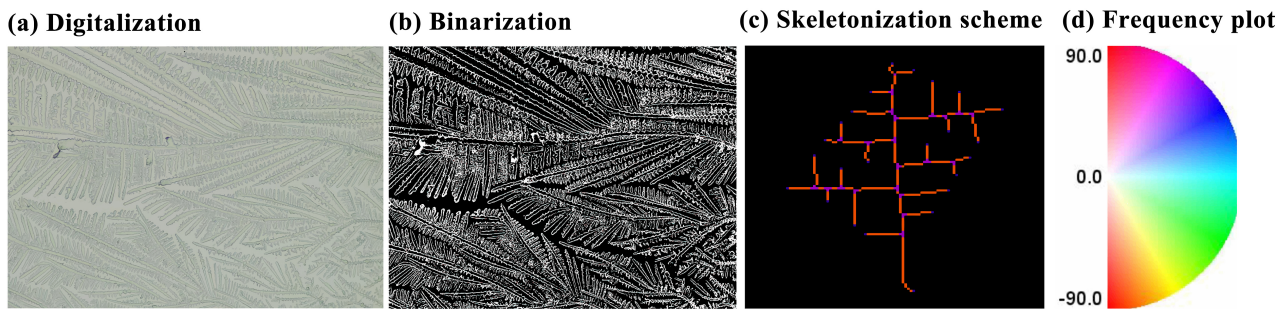


Fig. 1. Digitization, binarization, skeletonization and crystallization directionality study. (a) Digitalization. Digitization was performed with a Motic Pantera digital microscope at 200–300 magnification, after optical evaluation of crystallization with an XSZ-H optical microscope at 200–300 magnification. (b) Binarization. A scan of the digital matrix of the image was performed to obtain the reduction of the greyscale in binary values. (c) Skeletonization scheme. The skeletonization allowed us to reduce the binary regions of the image to a skeletal remnant while preserving the original extension and connectivity of the branches, and the directionality of the branches using the Fourier function was then performed. In the image obtained it was studied up to 22 joints between branches (fuchsia) and 24 branch ends (purple). (d) Frequency plot. The angles obtained were plotted in frequency histograms, and they were represented according to the average frequencies obtained in color taking into account the coloration of the angles of the chromatic disc.

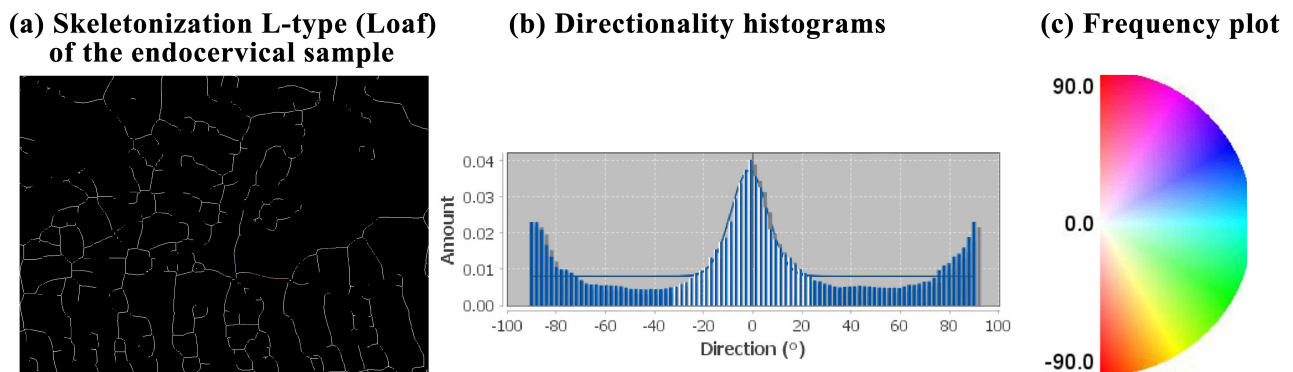


Fig. 2. Main Outcome Measure. (a) Skeletonization L-type (Loaf) of the endocervical sample. The L-type endocervical skeletonization corresponds to a 300 magnification of the crystallization zone of the main branch. (b) Directionality study. Two symmetrical peaks at 90 degrees in their absolute value are observed in the histogram, and a third group is between -20 and $+20$ degrees, which is equidistant to the maximum peak at 0 degrees, and perfectly defines a right-angled branch. The average absolute value directionality of branch connections is around 90 degrees. With this data, the color describes the frequencies of the directionality. (c) Frequency plot. Two color populations that define right-angled branches are identified, between blue-green and red-orange colors. This distribution in branch coloration represents the most frequent angles found around the central axis that have a preferentially right-angled orientation.

evaluate the classification of the directionality of the computational computer study of the crystallization of the samples obtained by vulvovaginal secretion. For this purpose, the directionality of a sample within the endocervical canal, not within the endocervical crypts, was considered as the primary outcome measure to contrast with the samples obtained by vulvovaginal secretion.

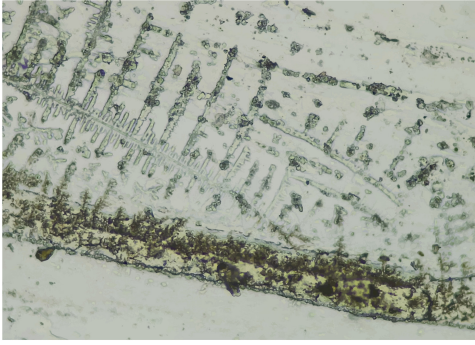
2.4 Criteria for Establishing Main Outcome Measure

For the study, a sample of endocervical, high-quality symmetry branching was included, as can be seen in Fig. 2.

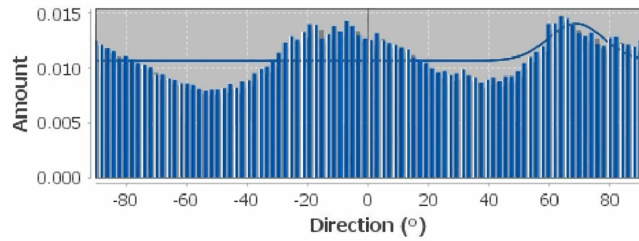
The endocervical sample was taken with a Novack curette after placing a speculum in the patient. The secre-

tion was aspirated from inside the cervical canal without curettage of the endocervix. The liquid sample was spread on a glass slide and allowed to air dry. The main endocervical capture sample result was the closest to the P day and was considered the true positive control. The sample to obtain the reference value was taken closest to the P day, in the interval $[\text{Midpoint} - P]$ in FW $[-6P - (\text{Midpoint}) - P]$. The sample was taken on day 15 of the menstrual cycle corresponding to the intracervical sample crystallization areas in the interval $(\text{Midpoint} - P) 10 \text{ KL}$. The distribution of the orientation of the branches of the capture performed was made from an endocervical crystallization type L which is distributed in 3 populations as shown in Fig. 2.

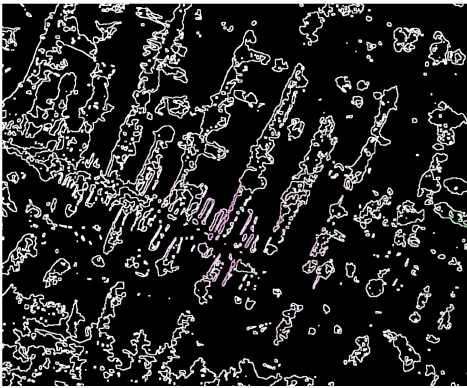
(a) Binarization



(b) Directionality histograms



(c) Skeletonization and coloration



(d) Frequency plot

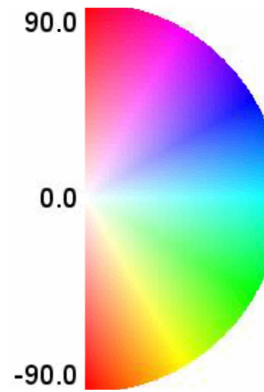


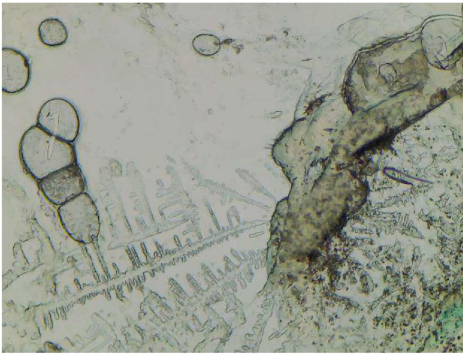
Fig. 3. Binarization, skeletonization and staining of crystallization frequencies. (a) Binarization. The figure corresponds to the binarization of the scan of digital image. (b) Directionality histogram. (b) shows the frequency histogram and the relationship between the distribution of the histogram and the most preferred frequencies, which is observed in three populations. (c) Skeletonization and coloration of crystallization frequencies. The color representation of the angles in the skeletonized figure takes the form of two populations of colors representative of the orientation of the population of angles that occur most frequently in fuchsia and green. (d) Frequency plot. (d) corresponds to the frequency angles on the chromatic disk to indicate the color relationship of the crystallization angles analyzed by the frequency histogram.

Fig. 2 shows the distribution of the frequency study on three populations of preferred angles obtained from the typical endocervical crystallization of an L-type secretion, corresponding to the digitalization and binarization of Fig. 1a,b respectively. Two color populations defining right angle branches between blue-green and red-orange colors are identified as can be seen in Fig. 2a. This distribution in branch coloration represents the most frequent angles found around the central axis that have a preferentially right-angled orientation. Therefore, the mean directionality in its values is composed of the conjunction of branches around 90 degrees, if we consider the frequency histogram, where we can say that it is a right-angled branch. The mean frequency histogram shows the first mean frequency distribution plotted with an orientation of 90 degrees, as shown in Fig. 2b.

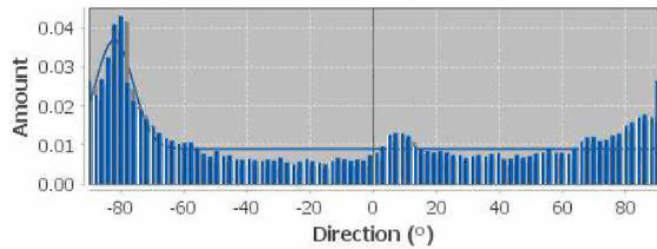
3. Results

A total of 29 captures were selected for analysis, of which 58.6% were positive as true positives. Thirty-four percent were true negatives, and 6.8% represented 2 cases in which they were falsely identified due to unstructured areas and were therefore erroneously classified as positives. No cases were identified as false negatives. This statistical difference was significant with a Chi-Square p test (< 0.001). Four samples corresponding to Figs. 3,4,5,6 classified in the true positive group are described in detail below. A detailed description of the result of a sample with a flat histogram is also included. The present selection of images is intended to show the characterization of the pattern found positive when compared to the directionality study of the main outcome of the measure. Fig. 3a shows the binarization of the scanned image, and Fig. 3b shows the corresponding histogram of frequencies distributed in three populations. A typical three-frequency pattern is observed, far from being isotropic. The mean frequency distribution starts in this

(a) Digitalization area



(b) Directionality histograms



(c) Color skeletonization



(d) Frequency plot

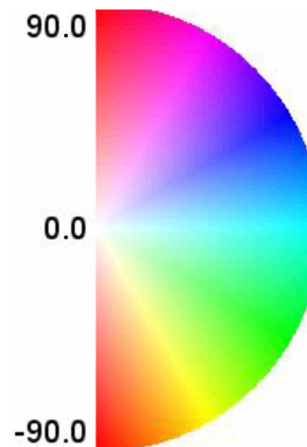


Fig. 4. Digitalization area, frequency diagram and colour diagram of the frequency angles obtained in the skeletonization process. (a) Digitalization area. (a) shows the scanned area. (b) Directionality histogram. (b) shows a histogram shifted at -80 degrees defining the preferred histogram population, characteristically marked at an angle close to 90 degrees to the branch axis. (c) Color skeletonization. The orange shading in the color range corresponds to -80° angles, as reflected in the central axis branch. (d) Frequency plot. (d) corresponds to a color disk to represent the angles of the frequency histogram.

case from 55 degrees and has a maximum peak of mean distribution around 70 degrees in the Gaussian curve description. Another group observed was formed by a symmetric population opposite to this group of frequencies with a mean frequency peak at -90 degrees, and a third population in the center representing the central branch, with a frequency peak between (-10 and $+10$ degrees). In Fig. 3c, the angle color of the skeletonized figure plots results in two representative right-angle populations in fuchsia and green, according to the histogram directionality that determines a right-angle orientation.

Fig. 4a shows a preferred group of angles analyzed in the histogram at -90° , as can be seen in Fig. 4b. The corresponding orange coloring on the color scale can be observed, which corresponds to angles with a mean frequency range of -80° , as reflected in the right-angle skeleton diagram on the central axis branch in Fig. 4c.

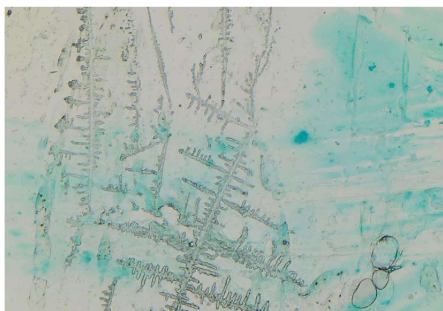
The histogram in Fig. 5b shows similar behavior in

the distribution of the preferred frequencies of the three populations. Two groups of preferred frequencies are observed with a maximum peak at 90° , and another symmetrical around an axis at -20° as can be seen in Fig. 5b. Two preferred shades, green and fuchsia, are identified in Fig. 5c, corresponding to 90° angles.

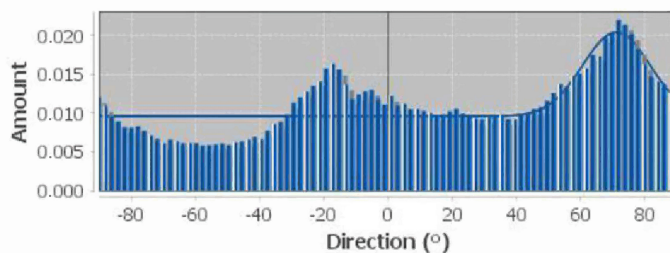
The latter sample is characteristically organized around the central axis of the highest frequency and vertical orientation around 0° , as seen in Fig. 6a,b. The frequency symmetry corresponding to the green-fuchsia staining is due to the relationship with the branches perpendicular to the central axis, as shown in Fig. 6c.

The study of Fig. 7a reveals a fully flat histogram, without any preference for directionality, as seen in Fig. 7b. The color representation of the angles obtained from the skeletonization reveals a collage of colors in different orientations according to the colorimetry of Fig. 7c. In this sample, it can be said that it does not correspond to a 90°

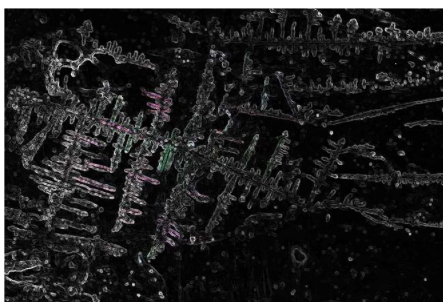
(a) Digital image scanning



(b) Directionality histograms



(c) Color skeletonization



(d) Frequency plot

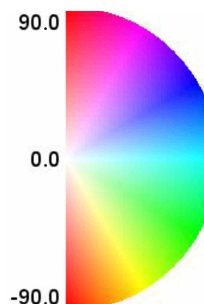


Fig. 5. Digitalization area, crystallization frequencies and colour skeletonization. (a) Digital image scanning. The figure corresponds to the scanning of the digital image. (b) Directionality histogram. In this case, the population of preferred frequencies is greater than 75 degrees and two more frequency groups are observed; with a maximum peak at -90 degrees, and another asymmetric around the axis at -20 degrees, which tends to a preferred right-angle orientation as seen in the coloration of the (c) Color skeletonization. The chromatic skeletonization of the scanned sample represents two preferred colors, green and fuchsia which are observed at right angles. (d) Frequency plot. (d) corresponds to the color disc representing the angles of the frequency histogram.

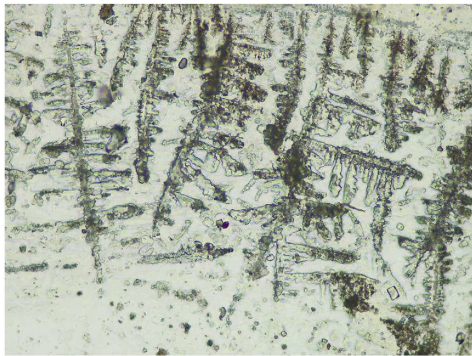
degree pattern, which could be representative of a type G secretion. Fig. 7d makes it possible to observe practically all the colors observed from various angles, since there are no preferred frequencies, so practically all the colors of the color discogram are represented, which coincides with the absence of a preferred branching pattern. It has not been possible to find samples of other characteristics in the vulvovaginal discharge in this series.

4. Discussion

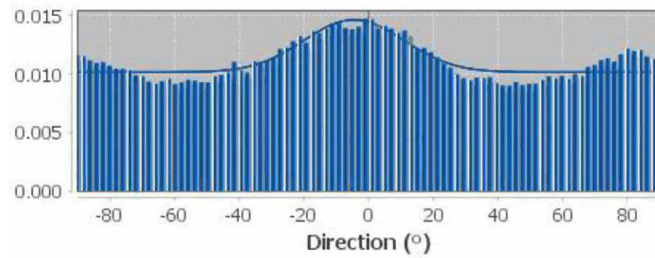
The skeletonization of an image of the crystallization of vulvovaginal discharge in this series allows us to identify three mean frequencies in the pattern of behavior of L-type samples. A definite pattern in FW is observed both in the study of the histogram angle frequencies and in the coloration of the branches, which follow an ordered pattern with a tendency to be perpendicular to 90 degrees. The four samples labeled with the numbers 3, 4, 5, and 6 show a similar behavior compared to the endocervical sample. Thus, this study of the directionality of branch connection of a cervical crystallization allows us a methodology to verify the L-type secretion in the vulvovaginal discharge. Sample 7 reveals a histogram with no preferred directionality. Looking at the skeletonization of the capture with the angles

being recorded, a collage of colors in different directions is seen, which is characteristic of a lack of internal organization in the directionality of the angles and mixing of colors in the face of the impossibility of detecting a preferred angle. This pattern may be characteristic of a sample without symmetry, which could be characteristic of a G-type sample. In Fig. 7a, the attached digitized image reflects a capture with a type of branch that simulates an L-type secretion. These findings are well known in FW according to Odeblad's scheme [24,32]. G-type crystallization according to this scheme is also found in FW. Therefore, a smoothed multi-frequency curve with a flat histogram may be characteristic of a G-type secretion as seen in this figure. This sample may correspond to intermediate shots with part of mucus type L and G. This would explain the mixture of colors and angles in the same shot. It could be predicted that outside the fertile window, the absence of an orderly orientation of the branches is characteristically higher, which would allow us to see multicolored skeletonization with no established pattern. Outside the FW we know that a type G pattern is more frequently identified according to the Odeblad's scheme. Further studies could be performed to verify the presence of this previously described multicolor pattern outside the fertile window [24,32].

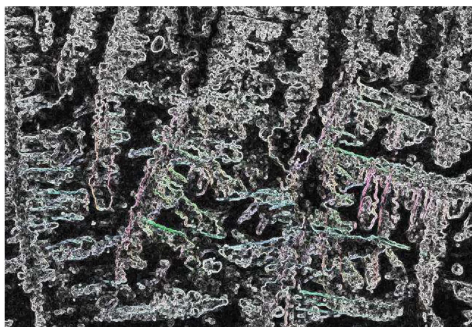
(a) Digitalization of the crystallization



(b) Directionality histograms



(c) Color skeletonization



(d) Frequency plot

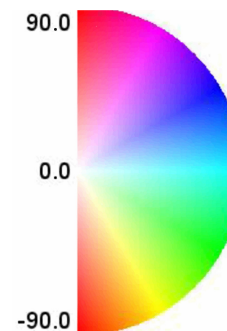


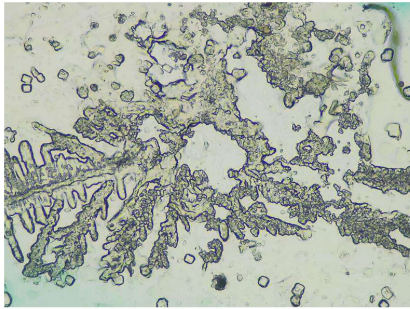
Fig. 6. Digitalization area, frequency diagram and colour diagram of the frequency angles obtained in the skeletonization process. (a) Digitization of the selected crystallization zone. (b) Directionality histogram. (b) is characteristically organized around the central axis of higher frequency and vertical orientation around 0 degrees. It represents a set of branches characteristically demonstrating two symmetrical populations at the extremes of the maximum peak at 80 and -80 degrees, symmetrical with a central group between (-20 and 20 degrees) of the maximum peak at zero degrees. (c) Color skeletonization. A right-angle orientation representative of the histogram is observed in the skeletonization coloration. Both preferred frequencies in red and blue-green colors represent respectively histogram angles of preferably perpendicular orientation (d) Frequency plot: The colors of the preferred angles are observed on the color disc.

We have used the CrMS to record FW days in the collected vulvovaginal samples. However, other classifications exist to study changes in the pattern of cervical secretion throughout the cycle [15–18]. The billing method is another way to identify the FW, but in this series, it was impossible, not because of the method, but because of the technical difficulty described above in this series.

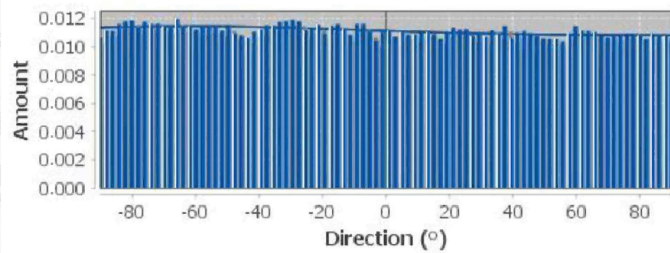
In this study, all samples were possible to integrate into the FW interval, which allowed us in this short series to integrate the observational branched crystallization patterns of the samples taken in the study. Under physiological conditions, the characteristic “fern-leaf” arborization is proportional to the circulating estradiol concentration and therefore maximal in the preovulatory phase [21–24,29–34]. The distinctive changes of each phase can only be determined and characterized by mixing the percentages of the different crystallization patterns by microscopy, but this is only possible in an endocervical sample according to Odeblad’s scheme [32]. A quantifiable stage-by-stage characterization of the crystallization of cervical secretion was

not possible by studying a cervical discharge sample. This series has allowed us, by studying the skeletonization, binarization, and directionality of a crystallized image to identify the mean frequencies that are repeated in the behavioral pattern of L-type samples. A definite pattern was observed in the FW in the study of the angular frequencies of the histogram and in the coloration of the branches, which follow an ordered pattern with a tendency to be perpendicular to 90 degrees. Therefore, we were able to see, a representative orientation of the right-angled histogram characteristic of 3 groups of populations of the studied angles, demonstrating the perpendicular relationship of the same, thus it was possible to differentiate this comparison by applying the comparison model of a perfect branch comparison sample of endocervical origin. The main outcome sample for this study was taken from endocervical sampling, which describes a 90-degree arborization within the cervical canal. It was the way to verify that the samples obtained for vulvovaginal crystallization have their origin in endocervical secretion.

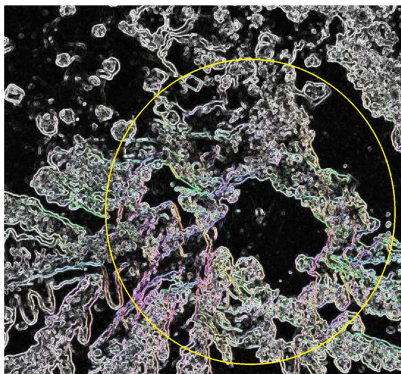
(a) Digitalized crystallization sample



(b) Directionality histograms



(c) Collage in the skeletonization



(d) Color discogram

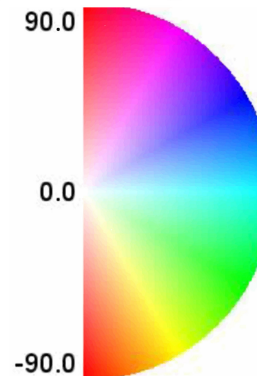


Fig. 7. Scanned crystallization image, directionality of the obtained frequencies and skeletonization of the image. (a) Digitalized crystallization sample. (a) is another digitalized sample of the vaginal discharge of cervical secretion. In this case, an atypical area was selected which does not correspond to a crystallization organized around an axis. The zone framed by the yellow circle was studied. (b) Directionality histogram. (b), reveals a histogram with no preferential directionality in the direction of the sample, and no frequency peak can be detected. (c) Collage of coloration obtained from the skeletonization study. When observing the coloration of the skeletonization of the capture of the angles in (c), a collage of colors is recorded in different directions according to the colorimetric scale. In this sample, it can be said that characteristically it does not correspond to a 90-degree pattern, and it could be compatible with a type G sample. (d) Color discogram. (d) makes it possible to observe practically all the colors observed from various angles, since there are no preferred frequencies, so practically all the colors of the color discogram are represented, which coincides with the absence of a preferred branching pattern.

It is well known that the volume of cervical secretion increases near the periovulatory period, with the greatest amount of secretion being observed around day -1 and 0 relative to EDO. Therefore, it is likely that it is possible to find this type of discharge in the middle of the cycle [35]. Finally, with this work, we have tried to present a scan in which the elasticity and transparency of the cervical secretion integrated with crystallization can be evaluated. The patterns of crystallization frequencies found depend on the ultrastructure of the crystallization of the glycoprotein network of the cervical crypts in hormonal response [32]. Thus, in this short series, we have been able to integrate the characteristics of the fluidity of cervical secretion in the pre-ovulatory phase with the observed pattern of crystallization. Standardized characterization of these findings may be the subject of future developments, since the fluidity, elasticity, and transparency of cervical secretion is quantifiable,

and are modified with hormonal changes allowing the detection of biophysical changes in cervical secretion.

However, it may be possible to use another reference point to identify the P day, such as ultrasound, the LH urine test, basal temperature if used appropriately, or isolated biophysical markers. The purpose of this brief study was to present the observation of cervical crystallization in FW. It can become an observable parameter in subfertile patients in order to aid in becoming pregnant. The crystallization process is an inexpensive and easily accessible technology for use by the general public.

5. Conclusions

In this study of the digitization of the crystallization of cervical secretion, we were able to identify a 90-degree L-type pattern in the FW. Considering the branching angles studied in the directionality study of the crystallization of

cervical secretions, the presence in the histogram of right-angled frequencies allowed us to recognize the L-type pattern of cervical secretion. The skeletonization of the studied images together with a FW indicator allowed us to identify this crystallization pattern in samples at the local level in vulvovaginal secretion. Therefore, it was possible to recognize L-type secretion as a biomarker in vaginal discharge samples in FW.

The possibility of adding more data to the fertility diagnostic process may be worthwhile to help determine the most fertile days of FW by simply studying vulvovaginal secretions. This information could be useful for subfertile patients looking for a simple biomarker to help recognize the peak fertility time within FW.

Availability of Data and Materials

The data sets used and/or analyzed during the present study are available upon reasonable request and describing the reason to the corresponding author.

Author Contributions

JMML conceived the study and drafted the original manuscript, performed the conceptualization and the main analyses of the manuscript. JMML, CR and MLEE contributed to data acquisition. JS, MLEE, CR, JLA, MÁMC and OMM contributed to the conceptualization. JMML, MÁMC, OMM and JLA contributed to the analysis and interpretation of the data and statistical analysis. JMML and JS proofread and edited in preparation of the final draft. JMML, MÁMC and OMM made final adjustment of the graphic design. All authors contributed to editorial changes in the manuscript. All authors read and approved the final manuscript. All authors have participated sufficiently in the work and agreed to be accountable for all aspects of the work.

Ethics Approval and Consent to Participate

The subject gave their informed consent for inclusion before they participated in the study, which was conducted in strict accordance with the Declaration of Helsinki, and whose protocol was approved by the Ethics Committee of CEImLAR, Center for Biomedical Research of La Rioja (CIBIR) (approval number P.I.339).

Acknowledgment

We would like to thank all those who helped us during the construction of this manuscript, in special in the process of capturing images of digitalization by the microscopy of anatomy pathological laboratory.

Funding

This research received no external funding.

Conflict of Interest

The authors declare no conflict of interest. José María Murcia Lora and Juan Luis Alcázar are serving as one of the Guest editors of this journal. We declare that José María Murcia Lora and Juan Luis Alcázar had no involvement in the peer review of this article and has no access to information regarding its peer review. Full responsibility for the editorial process for this article was delegated to Luca Roncati.

References

- [1] Taylor H, Pal L, Seli E. *Speroff Endocrinología ginecológica clínica y esterilidad*. 9th edn. Wolters Kluwer: Alphen aan den Rijn, Netherlands. 2021.
- [2] McNeilly AS, Crawford JL, Taragnat C, Nicol L, McNeilly JR. The differential secretion of FSH and LH: regulation through genes, feedback and packaging. *Reproduction* (Cambridge, England). Supplement. 2003; 61: 463–476.
- [3] Holesh JE, Bass AN, Lord M. *Physiology, Ovulation*. StatPearls Publishing: Treasure Island (FL). 2022.
- [4] Behre HM, Kuhlage J, Gassner C, Sonntag B, Schem C, Schneider HP, *et al.* Prediction of ovulation by urinary hormone measurements with the home use ClearPlan Fertility Monitor: comparison with transvaginal ultrasound scans and serum hormone measurements. *Human Reproduction*. 2000; 15: 2478–2482.
- [5] Check JH, Choe JK. Maximizing correction of infertility with moderate to marked diminished egg reserve in natural cycles by up-regulating follicle stimulating hormone receptors. *Gynecology & Reproductive Health*. 2022; 6: 1–7.
- [6] Check JH. Understanding the physiology of folliculogenesis serves as the foundation for perfecting diagnosis and treatment of ovulatory defects. *Clinical and Experimental Obstetrics & Gynecology*. 2012; 39: 273–279.
- [7] Barrett JC, Marshall J. The risk of conception on different days of the menstrual cycle. *Population Studies*. 1969; 23: 455–461.
- [8] Schwartz D, Macdonald PD, Heuchel V. Fecundability, coital frequency and the viability of Ova. *Population Studies*. 1980; 34: 397–400.
- [9] Royston JP. Basal body temperature, ovulation and the risk of conception, with special reference to the lifetimes of sperm and egg. *Biometrics*. 1982; 38: 397–406.
- [10] Fehring RJ, Schneider M. Variability in the hormonally estimated fertile phase of the menstrual cycle. *Fertility and Sterility*. 2008; 90: 1232–1235.
- [11] Stanford JB, Parnell T, Kantor K, Reeder MR, Najmabadi S, Johnson K, *et al.* International Natural Procreative Technology Evaluation and Surveillance of Treatment for Subfertility (iNEST): enrollment and methods. *Human Reproduction Open*. 2022; 2022: hoac033.
- [12] Stanford JB, Willis SK, Hatch EE, Rothman KJ, Wise LA. Fecundability in relation to use of mobile computing apps to track the menstrual cycle. *Human Reproduction*. 2020; 35: 2245–2252.
- [13] Guida M, Bramante S, Acunzo G, Pellicano M, Cirillo D, Nappi C. Diagnosi di fertilità con l'impiego di un test domestico di valutazione ormonale. *Minerva Ginecologica*. 2003; 55: 167–173. (In Italian)
- [14] Ecochard R, Duterque O, Leiva R, Bouchard T, Vigil P. Self-identification of the clinical fertile window and the ovulation period. *Fertility and Sterility*. 2015; 103: 1319–1325.e3.
- [15] Billings EL, Brown JB, Billings JJ, Burger HG. Symptoms and hormonal changes accompanying ovulation. *Lancet*. 1972; 1: 282–284.

- [16] Duane M, Stanford JB, Porucznik CA, Vigil P. Fertility Awareness-Based Methods for Women's Health and Family Planning. *Frontiers in Medicine*. 2022; 9: 858977.
- [17] Fehring RJ. Accuracy of the peak day of cervical mucus as a biological marker of fertility. *Contraception*. 2002; 66: 231–235.
- [18] Scarpa B, Dunson DB, Colombo B. Cervical mucus secretions on the day of intercourse: an accurate marker of highly fertile days. *European Journal of Obstetrics, Gynecology, and Reproductive Biology*. 2006; 125: 72–78.
- [19] Bigelow JL, Dunson DB, Stanford JB, Ecochard R, Gnath C, Colombo B. Mucus observations in the fertile window: a better predictor of conception than timing of intercourse. *Human Reproduction*. 2004; 19: 889–892.
- [20] Wilcox AJ, Weinberg CR, Baird DD. Timing of sexual intercourse in relation to ovulation. Effects on the probability of conception, survival of the pregnancy, and sex of the baby. *The New England Journal of Medicine*. 1995; 333: 1517–1521.
- [21] Odeblad E. The functional structure of human cervical mucus. *Acta Obstetrica et Gynecologica Scandinavica*. 1968; 47: 57–79.
- [22] Odeblad E. The biophysical properties of the cervical-vaginal secretions. *International Review of Natural Family Planning*. 1983; 7: 1–56.
- [23] Odeblad E. The biophysical aspects of cervical mucus. In Jordan J.A.; Singer A (eds.) *The cervix* (pp. 45–58). WB Saunders: London. 1976.
- [24] Odeblad E. Micro-NMR in high permanent magnetic fields. Theoretical and experimental investigations with an application to the secretions from single glandular units in the human uterine cervix. *Acta Obstetrica et Gynecologica Scandinavica*. 1966; 45: Suppl 2:1–188.
- [25] Moghissi KS. Sperm migration through the human cervix. In Elstein M.; Moghissi K.S.; Borth R. (eds.) *Cervical mucus in human reproduction* (pp. 128–151). Scriptor: Copenhagen. 1973.
- [26] Hilgers, Thomas W. *The Medical & Surgical Practice of NaProTechnology*. 1st edn. Pope Paul VI Institute Press: Omaha, Nebraska, USA. 2004.
- [27] Stanford JB, Carpentier PA, Meier BL, Rollo M, Tingey B. Restorative reproductive medicine for infertility in two family medicine clinics in New England, an observational study. *BMC Pregnancy and Childbirth*. 2021; 21: 495.
- [28] Murcia JM. Multidisciplinary Fertile Window Assessment for Ovulation Diagnosis. *Academia Letters*. 2021; 2.
- [29] Menárguez M, Pastor LM, Odeblad E. Morphological characterization of different human cervical mucus types using light and scanning electron microscopy. *Human Reproduction*. 2003; 18: 1782–1789.
- [30] Portales PV, Cortés MEC. Fractality in a pattern of crystallization of human cervical mucus obtained at periovulatory period. *Revista Cubana de Investigaciones Biomédicas*. 2019; 38: 296–302.
- [31] Vigil P, Cortés ME. Cristalización y ultraestructura de la secreción cervical humana. *Acta bioquímica clínica latinoamericana*. 2020; 54: 337–338.
- [32] Odeblad E. The discovery of different types of cervical mucus and the Billings Ovulation Method. *Bulletin of the Natural Family Planning Council of Victoria*. 1994; 21: 3–34.
- [33] Adlercreutz H, Brown J, Collins W, Goebelsman U, Kellie A, Campbell H, *et al.* The measurement of urinary steroid glucuronides as indices of the fertile period in women. World Health Organization, Task Force on Methods for the Determination of the Fertile Period, special programme of research, development and research training in human reproduction. *Journal of Steroid Biochemistry*. 1982; 17: 695–702.
- [34] Curlin M, Bursac D. Cervical mucus: from biochemical structure to clinical implications. *Frontiers in Bioscience-Scholar*. 2013; 5: 507–515.
- [35] Murcia JM, Martínez O, Simoni J, Calvo MM, Falces A, Mejía JE, *et al.* Fertile window and biophysical biomarkers of cervical secretion in subfertile cycles: a look at biotechnology applied to NaProTechnology. *Clinical and Experimental Obstetrics & Gynecology*. 2022; 49: 17.